RL-Course 2024/25: Final Project Report

Karahan Sarıtaş, Kıvanç Tezören, Oğuz Ata Çal
Muhteshember
`University of Tübingen`

February 26, 2025

1 Introduction

In this project, we aim to develop a reinforcement learning agent capable of achieving a competitive performance in a 2-player hockey game environment (which inherits from `gym.Env`), simulated with Box2D physics engine. Each player controls a hockey stick and tries to score goals with a puck. Our observation space consists of 18 dimensions: position (x and y), velocity (x and y), angle and angular velocity of both players, position and velocity (x and y) of the puck, and remaining times for players to hold the puck (if `keep_mode` is set to `True`, otherwise players cannot hold the puck).
Actions in this environment are similarly represented by a list of four floats: change of direction in x and y coordinates, clockwise or counter-clockwise rotation, and shooting a puck. Agents can also pick and carry the puck before shooting. The environment rewards the player agent's closeness to puck in each frame, and additionally incurs a penalty of -10 or an additional reward of 10 in case of a loss or win, respectively.
For this problem, we implemented the following reinforcement learning algorithms:

- **Soft Actor-Critic (SAC)**, implemented by Karahan Sarıtaş,
- **Deep Q-Networks (DQN)**, implemented by Kıvanç Tezören.
- **Twin Delayed Deep Deterministic Policy Gradient (TD3)**, implemented by Oğuz Ata Çal,

These algorithms were chosen because of the diversity of their principles and their comparable performance.

2 Method

2.1 SAC: Soft Actor-Critic

SAC is an off-policy algorithm that learns from a replay buffer, which contains experiences collected by the agent over time from different versions of the policy. To solve the exploration-exploitation dilemma, the policy is trained to maximize a trade-off between expected return and entropy. By incorporating entropy maximization into its objective function, SAC encourages exploration through stochastic behavior while also learning to act optimally. The entropy term helps prevent early convergence to suboptimal deterministic policies and allows the agent to discover multiple successful strategies. First, let's formulate the entropy of the policy $\pi(\cdot \mid s_t)$:

$$\mathcal{H}(\pi(\cdot \mid s_t)) = \mathbb{E}_{a\sim\pi(\cdot|s_t)}[-\log(P(\pi(a \mid s_t))] \tag{1}$$

In entropy-regularized reinforcement learning, the agent's objective is augmented with an entropy term. At each timestep, in addition to the environmental reward, the agent receives a bonus proportional to its policy's entropy, encouraging it to maintain stochastic behavior while learning optimal actions. Then the optimal policy is formulated as follows:

$$\pi^* = \arg\max_{\pi} \mathbb{E}_{\tau\sim\pi}\left[\sum_{t=0}^{\infty}\gamma^t\left(R(s_t, a_t, s_{t+1}) + \alpha\mathcal{H}(\pi(\cdot|s_t))\right)\right] \tag{2}$$

In the objective function, α serves as a temperature parameter that controls the balance between reward maximization and entropy maximization. A higher α value places more emphasis on exploration through entropy maximization, while a lower value prioritizes reward maximization. This parameter can either be set as a fixed hyperparameter or automatically adjusted during training to achieve a desired target entropy level.

Extension (1): Automating Temperature Tuning

The optimization problem for finding the optimal temperature variable is given as follows [7]:

$$\alpha_t^* = \arg\min_{\alpha_t} \mathbb{E}_{\mathbf{a}_t\sim\pi_t^*}\left[-\alpha_t \log \pi_t^*(\mathbf{a}_t|\mathbf{s}_t;\alpha_t) - \alpha_t\mathcal{H}_0\right] \tag{3}$$

Here $\mathcal{H}_0$ represents the predefined minimum policy entropy threshold. Authors of the same paper [7] choose $-\dim(\mathcal{A})$ as the target entropy, where $\mathcal{A}$ represents the action space. During the implementation, we have to make sure that the temperature variable α is positive. One way to do it is to optimize $\log(\alpha)$ instead of α. To ensure numerical stability, the authors chose to optimize a modified version of the objective function above where they replaced the exponent with directly the $\log\alpha_t$ - which doesn't affect the outcome of the objective function[1]. We followed the same approach in our implementation.

Extension (2): Prioritized Experience Replay (PER)

Normally, the transitions are uniformly sampled from a replay memory. Schaul et al. [12] introduces a new sampling strategy called Prioritized Experience Replay (PER) where we sample the important transitions more frequently. We prioritize the transitions from which our agent can learn significantly, by estimating the importance of a transition with TD error. Transitions with larger errors provide more valuable learning opportunities for the agent, as they represent cases where its predictions deviate significantly from actual outcomes.In alignment with the proportional prioritization proposed in the original paper [12], we adopt the "sum tree" data structure, which is a specific type of segment tree[2].

Extension (3): Pink Action Noise

Actions are sampled applying $\tanh$ squashing and rescaling to $x_t = \mu(s_t)+\sigma(s_t)\odot\epsilon_t$ where ϵ_t represents the action noise for better exploration. Most commonly, a Gaussian distribution (white noise) is called to generate actions during training. Eberhard et al. [4] introduces a new action noise called colored noise where the signals ϵ_t drawn from it satisfy the following property, $|\hat{\varepsilon}(f)|^2 \propto f^{-\beta}$ where $\hat{\varepsilon}(f) = \mathcal{F}[\varepsilon_t](f)$ corresponds to the Fourier transform of ϵ_t (f is the frequency) and $|\hat{\varepsilon}(f)|^2$ is called the power spectral density (PSD). β represents the color parameter. [4] empirically shows that the pink noise ($\beta = 1$) performs on par with the best choice of noise type in 80% of cases. We incorporated colored noise, including the specific case of pink noise, in our implementation[3].

[1] https://github.com/rail-berkeley/softlearning/issues/37

[2] We use the Open AI implementation: https://github.com/openai/baselines/blob/master/baselines/common/segment_tree.py

[3] Original implementation of the pink noise is used: https://github.com/martius-lab/pink-noise-rl/tree/main/pink along with the Action Noise interface provided here: https://github.com/DLR-RM/

2.1.1 Experiments

We conduct experiments with different hyperparameters for the SAC algorithm. Each hyperparameter can influence others, but due to time constraints, we kept most (or all) of the remaining hyperparameters fixed while varying one at a time. We begin by examining the impact of α tuning compared to using fixed α values. We train and evaluate the model against the weak opponent where evaluation takes place every 200 episodes and lasts 100 episodes.
First, we evaluate different temperature values (α, the entropy coefficient) using a vanilla SAC model with normal action noise. Figure 1a demonstrates that higher temperature values, which encourage excessive exploration, fail to converge. Meanwhile, automatic tuning and no temperature ($\alpha = 0$) shows similar training characteristics in both pink noise and normal action noise. To better understand the impact of the absence of entropy regularization, we further tested it against a **strong** opponent, this time with both pink and normal action noises. As shown in Figure 1b, automatic tuning consistently accelerates convergence in both pink and white action noise settings. Notably, white noise without temperature fails to converge altogether. Based on these findings, we decided to use **automatic tuning for the entropy coefficient** (α) in our final model.

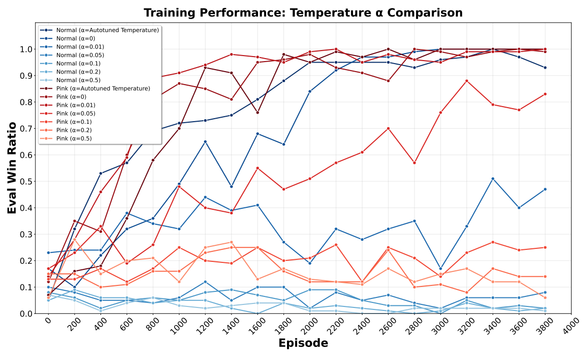

(a) Evaluation win rates against the weak opponent with different temperature values α

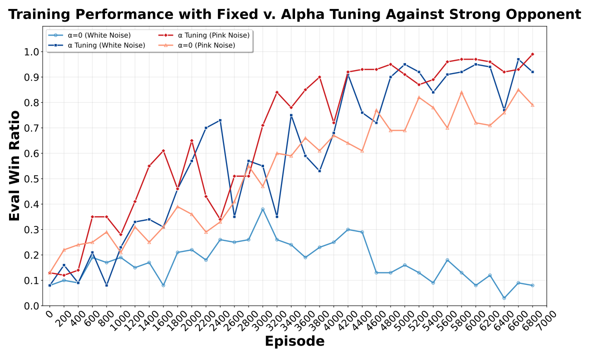

(b) Evaluation win rates against the strong opponent with different temperature values α

Figure 2a shows the performance of white noise, pink noise, and colored noise with $\beta = 0.75$ (as it was shown to achieve a competitive performance in [4]). We used both vanilla SAC and SAC with PER. Our experiment against weak opponent yields that although all the configurations lead to convergence, pink noise with vanilla SAC achieves the fastest convergence among all. As outlined in [14], SAC+PER introduces additional overhead on top of vanilla SAC due to constant priority updates and sampling computations, which scale linearly with the mini-batch size. Since SAC+PER takes longer to train and does not consistently outperform the baseline—Wang and Ross [14] also reports similar or worse performance in some environments—we choose to use **vanilla SAC with pink action noise**. Next, we tested different discount rates, which scale down the effect of past experiences. As shown in Figure 2b, we evaluated $\gamma \in \{0.95, 0.97, 0.99\}$ with both normal and pink action noise. The results indicate that the default value of $\gamma = 0.99$ achieves the fastest convergence, so we chose **0.99 as our discount rate**.
Next, we compare two different learning rates, $\eta \in \{3 \times 10^{-4}, 1 \times 10^{-3}\}$, using both pink and white action noise to assess their general impact on training. As shown in Figure 3a, reducing the learning rate to $\eta = 3 \times 10^{-4}$ (default) negatively affects training performance with pink noise against the weak opponent. Therefore, we chose $\eta = 10^{-3}$ for our final model. Final hyperparameter values are provided in Appendix Section A.1.

stable-baselines3/blob/master/stable_baselines3/common/noise.py

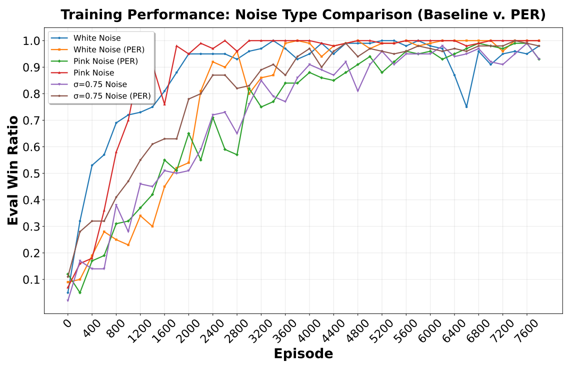

(a) Evaluation win rates against the weak opponent with different noise configurations

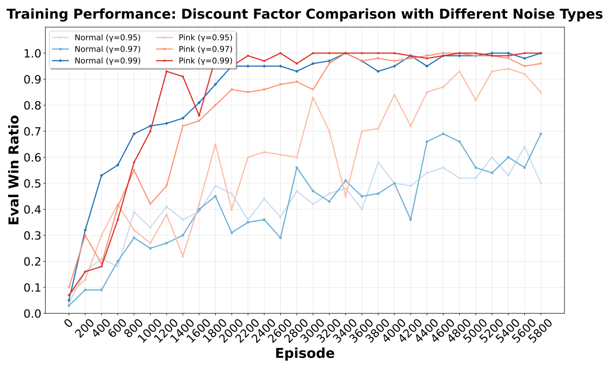

(b) Evaluation win rates against the weak opponent using different discounts (pink v. normal action noise)

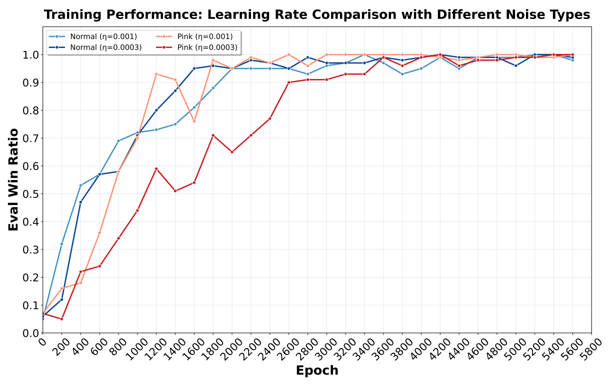

(a) Evaluation win rates against the weak opponent with different learning rates

Our hyperparameter search has limits: we couldn't do a full grid search due to resource constraints, and we used only one seed per experiment. However, Haarnoja et al. [6] suggests that the entropy coefficient α is the most critical hyperparameter to tune, while SAC is generally less sensitive to other hyperparameter choices. Since we have already addressed this by incorporating automatic α tuning, our focus now shifts to how we train our model, which we detail in the following section.

2.1.2 Training the Final Model

Mirrored States and Actions One observation we can do about our hockey environment is that it is symmetric with respect to a horizontal reflection (across the x-axis). This means that if we flip all the y-components (and the associated angles and y-velocities) of the state, we obtain an equivalent "mirrored" state. By using symmetry, our approach enables an agent to learn from both the original experiences and their mirrored counterparts, thereby fully exploiting the game's inherent symmetric structure.

Reward Augmentation Currently, the initial reward uses the outcome of the game (win/loss) and then adds a bonus based on how close the agent is to the puck. However, we can incorporate additional aspects of the game such as the direction of the puck and whether or not agent touches the puck. To do so we used a simple, augmented version of the reward, using the proxy rewards already provided by the environment:

$$\begin{aligned} r_{\text{aug}} = 0.5 \cdot \texttt{reward\_closeness\_to\_puck} &\quad + 2.0 \cdot \texttt{reward\_touch\_puck} \\ + 1.0 \cdot \texttt{reward\_puck\_direction} &\quad + r_{\text{w/l}}. \end{aligned}$$

where $r_{\text{w/l}}$ is +10 if our agent wins, -10 if it loses and 0 if the game ends with a tie.

Self-play: Prioritized Opponent Buffer The Prioritized Opponent Buffer[4] is used in self-play to store previously encountered opponents and select which one to face next based on Discounted UCB [8].

[4]Introduced by RLcochet from previous years.

Each time a new opponent appears, it is added to a list, and we keep a rolling history of size τ with the outcomes of the most recent matches. If the result of the t-th match is r_t (for example, $r_t = 1$ for a win or $r_t = 0$ for a loss), we apply a discount factor γ to favor more recent games. Specifically, the "discounted count" for opponent i is $N_i = \sum_{t=1}^{\tau} \mathbf{1}\{\text{opponent}_t = i\}\, \gamma^{(\tau - t)}$, and the discounted average outcome is $X_i = \frac{\sum_{t=1}^{\tau} r_t\, \mathbf{1}\{\text{opponent}_t = i\}\, \gamma^{(\tau-t)}}{N_i}$. The bonus is calculated as follows $c_i = 2B\sqrt{\xi\, \frac{\ln(\sum_j N_j)}{N_i}}$, and we pick the opponent i that maximizes $\text{score}_i = X_i + c_i$. This means opponents with worse performance (low X_i) or limited exposure (low N_i) receive more training attention, while still giving a chance to practice against others. After each match, the buffer updates its history with the chosen opponent and the outcome, allowing the next selection to adapt based on new results. We initialized POB with weak and strong opponents, along with different SAC and TD3 models trained with different settings (diverse reward augmentations, with our without symmetry, trained against weak/strong or in defense/shooting mode etc.). We aimed to increase the variety of playing techniques our final model was exposed to during training. Lastly, we started our self-play training with a model that was trained against the strong opponent for 10K episodes. For self-play with POB, we trained it for 200K episodes and updated the opponent for each 50 episodes if agent is able to achieve 0.95 win rate against everyone in the buffer - otherwise we just continue with the current agent. A pseudocode for the self-play with POB algorithm can be found in Appendix Section A.2.

3 Twin Delayed Deep Deterministic Policy Gradient (TD3) [5]

3.1 Method

Twin Delayed Deep Deterministic Policy Gradient (TD3) is an off-policy reinforcement learning algorithm that addresses some of the challenges in value-based methods while maintaining stable learning in continuous action spaces. Building upon the Deep Deterministic Policy Gradient (DDPG) framework, TD3 introduces three significant innovations to mitigate value overestimation bias and improve learning stability: clipped double Q-learning, delayed policy updates, and target policy smoothing.
The algorithm specifically tackles the overestimation bias inherent in Q-learning-based methods [13] through its twin critic architecture. TD3 maintains two separate Q-networks (Q_{ϕ_1} and Q_{ϕ_2}) with independent parameters, using the minimum of their estimates to form the target value:

$$y = r_t + \gamma \min_{i=1,2} Q_{\phi_{\text{targ},i}}(s_{t+1}, \tilde{a}_{t+1})$$

where $\tilde{a}_{t+1}$ is a noise-perturbed action from the target policy:

$$\tilde{a}_{t+1} = \pi_{\theta_{\text{targ}}}(s_{t+1}) + \epsilon, \quad \epsilon \sim \text{clip}(\mathcal{N}(0, \sigma), -c, c)$$

This target policy smoothing regularization prevents overfitting to narrow Q-value peaks by adding clipped noise to the target action. The actor π_θ is then updated to maximize the expected Q-value from the first critic network:

$$\nabla_\theta J(\theta) = \mathbb{E}_{s_t \sim \mathcal{D}} \left[\nabla_a Q_{\phi_1}(s_t, a)|_{a=\pi_\theta(s_t)} \nabla_\theta \pi_\theta(s_t) \right]$$

Another innovation in TD3 is the delayed policy update mechanism, where the actor and target networks are updated less frequently than the critics (2:1 update ratio in our implementation) allows for more stable Q-function learning before policy improvements. The complete algorithm can be split into the following components:

3.1.1 Extension: Pink Noise

Exploration noise helps prevent reinforcement learning models from getting stuck in suboptimal solutions. While white noise (like Gaussian noise) is common, using temporally correlated noise can make actions smoother and more natural. Pink noise, or $1/f$ noise, has lower frequencies that dominate its power, creating smoother, more gradual changes compared to white noise. This makes it useful in tasks where sudden changes can cause problems. Recent studies [4] show pink noise can improve exploration and control, making it a promising choice for certain tasks.

3.1.2 Extension: Random Network Distillation for Enhanced Exploration

Sparse or deceptive reward structures can be difficult for policy-gradient methods, as standard exploration strategies may not visit novel states enough. **Random Network Distillation** (RND) [3] provides an intrinsic reward that guides exploration toward unfamiliar regions of the state space. The approach uses two networks:
The **Target Network**, f_{rnd}, is a randomly initialized, fixed network that processes states and outputs a feature representation, with its parameters remaining unchanged during training. On the other hand, the **Predictor Network**, f_{pred}, is a trainable network with the same architecture as f_{rnd}, which learns to mimic the target network's outputs.
At each timestep, the intrinsic reward is computed as the squared error between the predictor's and target's outputs:

$$r_{\text{rnd}}(s_t) = \|f_{\text{pred}}(s_t) - f_{\text{rnd}}(s_t)\|^2.$$

Intuitively, rarely encountered states produce higher prediction errors, yielding larger intrinsic rewards that encourage exploration. As the predictor network learns these states, the error—and hence the intrinsic reward—decreases, preventing repeated exploitation of the same novelty.

Integration with TD3. To incorporate RND into TD3, the total reward is augmented by adding a scaled intrinsic reward to the environment's extrinsic reward: $r_{\text{total}} = r_t + \alpha_{\text{rnd}}\, r_{\text{rnd}}(s_t)$, where α_{rnd} controls the influence of intrinsic rewards. This combined reward drives both critic and actor updates in TD3. Empirically, RND has shown promise in tasks that require extensive state-space coverage, proving effective in both Atari and other domains [3, 9, 1].

3.1.3 Extension: Layer Normalization

Layer normalization [2] re-centers and rescales neuron activations within a layer. For a layer output $\mathbf{h} \in \mathbb{R}^d$, it computes $\hat{\mathbf{h}} = \frac{\mathbf{h}-\mu_h}{\sigma_h}\,\alpha + \beta$, where μ_h and σ_h are the mean and standard deviation of $\mathbf{h}$ (computed across the feature dimension), and α and β are learned parameters. Unlike batch normalization, which normalizes across a batch, layer normalization standardizes each sample's features. This makes the learning process more robust to outlier activations and exploding gradients, which is particularly useful in off-policy actor-critic methods like TD3, where replay buffer experiences can vary significantly. As a result, layer normalization stabilizes updates and often leads to faster convergence with less sensitivity to hyperparameter settings [10]. Layer norm was implemented between all layers of both the actor and critic networks.

3.2 Experiments

We conduct an ablation study to identify the most effective hyperparameters. Training is done against a weak opponent for 12,000 epochs, evaluating every 100 epochs over 1,000 matches to compute win rates.

A moving average with a window size of 3 smooths the curves. Training accuracy refers to performance against the weak opponent. Default hyperparameters and architecture details are in the Appendix.

3.2.1 Noise Experiments

First, we examine the impact of exploration noise, testing six noise configurations with a focus on pink noise. To ensure completeness, we include two additional β values. The key hyperparameters are f_{min}, which defines the minimum frequency component (higher values reduce low-frequency dominance), and β, which controls the spectral slope ($\beta = 1.0$ for standard pink noise, with higher values emphasizing lower frequencies). Other extensions are disabled.

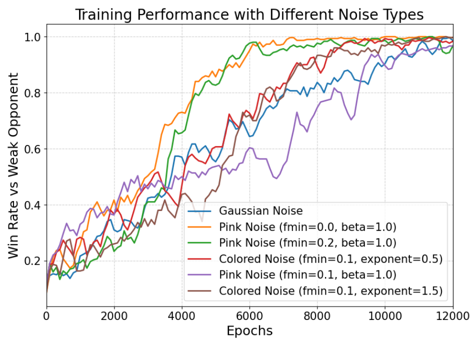

(a) Win Rates with Different Noise Types

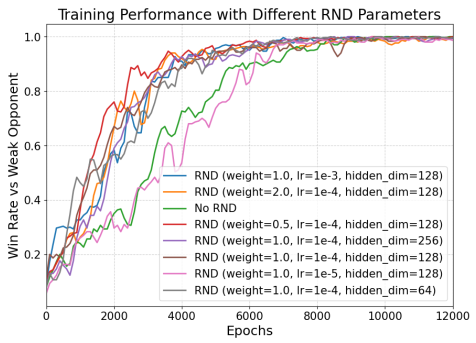

(b) Win Rates in RND Experiments

Figure 4: Comparison of Training Performance Across Noise and RND Experiments

As shown in Figure 4a, all experiments eventually overfit, achieving near-optimal performance. Thus, the key comparison is convergence speed. Pink noise with $f_{\text{min}} = 0.0$ and $f_{\text{min}} = 0.2$ improved the fastest, reaching a 0.95 win rate around 6000 epochs, while $f_{\text{min}} = 0.1$ lagged behind, failing to reach this threshold. Overall, $f_{\text{min}} = 0.0$ was the best-performing configuration, maintaining the highest win rate beyond 6000 epochs.

3.2.2 RND Experiments

We evaluate the impact of Random Network Distillation (RND) parameters on training performance, testing different weights, learning rates, and hidden dimensions against a no-RND baseline.
As shown in Figure 4b, RND accelerates convergence, with the no-RND baseline lagging behind until 7000 epochs. One of the best configurations with weight $= 1.0$, lr $= 10^{-3}$ and hidden dimension $= 128$ reaches the 0.95 win rate the fastest. Lower learning rates and smaller hidden layers slow learning, while excessively large ones offer no advantage. Overall, it can be said that RND improves learning efficiency.

3.2.3 Layer Normalization Experiments

In this study, we analyze the impact of LayerNorm with different ϵ values on training performance. We compare three settings ($\epsilon = 10^{-3}, 10^{-4}, 10^{-5}$) against a baseline without LayerNorm.
Results show that LayerNorm significantly accelerates convergence compared to the baseline, which lags behind until 7000 epochs. The best-performing configurations are $\epsilon = 10^{-3}$ and $\epsilon = 10^{-4}$, both reaching near-optimal win rates the fastest. $\epsilon = 10^{-5}$ shows slightly slower convergence but still outperforms the no-LayerNorm case. Overall, LayerNorm enhances learning speed, with $\epsilon = 10^{-3}$ providing the most stable and rapid convergence.

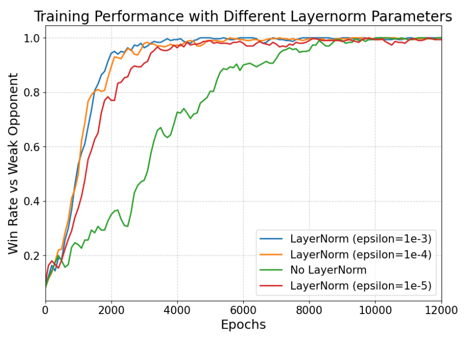

(a) Training Win Rates with Different Layernorm Parameters

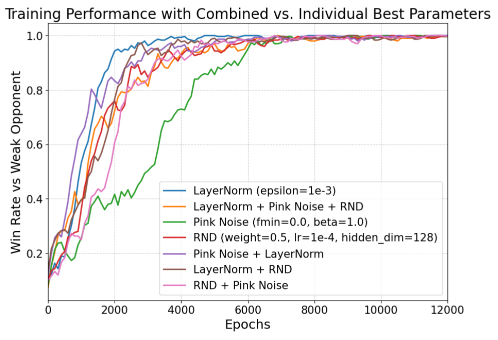

(b) Training Win Rates of Combined Best vs Individual Best Parameters

Figure 5: Comparison of Training Performance Across Noise and RND Experiments

3.2.4 Combining the Best Parameters

To assess whether combining the best-performing configurations yields further improvements, we trained agents using all combinations of LayerNorm ($\epsilon = 10^{-3}$), Pink Noise ($f_{\text{min}} = 0.0, \beta = 1.0$) and RND (weight $= 0.5$, lr $= 10^{-4}$, hidden dimension $= 128$). Figure 5b shows the result that the agent with just LayerNorm converges the fastest. As a result, the final agent for the tournament was trained using using only LayerNorm ($\epsilon = 10^{-3}$) against the weak and strong opponent, training and shooting sequentially for 100,000 episodes. Self-play was used to try to mitigate overfiting but ultimately it hindered performance so it was not used for the final agent.

3.3 DQN: Deep Q-Networks

In RL, functions of intractable action and state spaces are commonly encountered, including the action-value function $Q(s, a)$. The prevalent approach of approximating the optimal $Q^*(s, a)$ with a deep neural network was mainly introduced with Deep Q-Networks (DQN) [11].
DQN operates on a discrete action space $\mathcal{A} = \{a_1, ..., a_{|\mathcal{A}|}\}$. At each discrete time step t, the agent chooses an action $a_t \in \mathcal{A}$. Our implementation of the DQN action space is discussed in Section 3.3.4.
Let's recall how the optimal action-value function satisfies the Bellman equation and can be expressed recursively:

$$Q^*(s, a) = \max_{\pi} Q^{\pi}(s, a) = \max_{\pi} \mathbb{E}[R_t | s_t = s, a_t = a, \pi] = \mathbb{E}'_s[r + \gamma \max_{a'} Q^*(s', a') | s, a]$$

This allows for a DQN to approximate this function by a deep neural network: $Q(a, s; \theta)$ with parameters θ. Based on the recursive definition, the following sequence of loss functions can be minimized to learn the approximator [15]:

$$L_i(\theta_i) = \mathbb{E}_{s,a,r,s'} \left[\left(y_i^{DQN} - Q(s, a; \theta_i) \right) \right]$$

where i is the iteration number and the training objective is $y_i^{\text{DQN}} = r + \gamma \cdot \max_{\alpha'} Q(s', a'; \theta^-)$.
Here, θ^- represent the parameters of the "target network", which are kept fixed and updated once in every fixed number of iterations. Even though updating the target network each iteration is possible [11], in practice, this leads to a more instable training and a worse approximation [15]. Our experiments in Section 3.3.4 support these findings as well.

3.3.1 Extension (1): Double DQN

DQN's training objective y_i^{DQN} can provide overly-optimistic estimates as the $\max$ operator uses the same values for selecting and evaluating an action. Double DQN replaces this training objective with the following to compensate for possible over-estimations [13]:

$$y_i^{\text{DDQN}} = r + \gamma \cdot Q(s', \arg\max_{a'} Q(s', a';\, \theta_i);\, \theta^-)$$

Double DQN decouples action selection and evaluation by evaluating the selected action with the target network. The rest of the learning procedure is kept the same as DQN, and empirical results confirm that introducing Double Q-learning to DQN improves performance [13].

3.3.2 Extension (2): Dueling DQN

Based on the advantage function, which obtains a relative measure for each action's importance [15], the Dueling DQN architecture splits the Q estimator into two streams:

$$A^\pi(s,a) = Q^\pi(s,a) - V^\pi(s) \quad \Rightarrow \quad Q(s,a;\, \theta,\alpha,\beta) = A(s,a;\, \theta,\alpha) + V(s;\, \theta,\beta) \tag{4}$$

The main intuition behind this approach is to avoid evaluating the value of each action choice when it is not necessary [15]. The later fully-connected layers of the estimator are split into two streams capable of separately estimating the action and value functions. Their outputs are then merged to form the Q function estimation.
It is tempting to apply this merging step with summation as in Equation 4. However, this prevents the action and value functions from being recovered uniquely for a given Q, hampering the training. To ensure identifiability and thus improve performance, the estimator A is forced to have a zero advantage for the chosen action:

$$Q(s,a;\, \theta,\alpha,\beta) \approx \left(A(s,a;\, \theta,\alpha) - \frac{1}{|\mathcal{A}|}\sum_{a'} A(s,a';\, \theta,\alpha) \right) + V(s;\, \theta,\beta)$$

This arises from the fact that for an optimal action a^* maximizing Q (and thus A), $Q(s,a^*) = V(s)$ and thus $A(s,a^*) = 0$. The authors suggest that replacing the max operator with an average stabilizes the learning and improves the agent's performance in practice, even though it introduces an offset to the original learning target. We have implemented Dueling DQN using this form of the equation as well.

3.3.3 Extension (3): Prioritized Experience Replay

DQN uses experience replay, which provides data-efficiency as it re-uses experience [15]. As explained in Section 2.1, Prioritized Experience Replay (PER) changes the random sampling of experience replay by prioritizing experience based on their temporal difference error. This leads to faster and more accurate convergence during training in a variety of off-policy algorithms, including DQN agents [12, 15].

3.3.4 Experiments

Experiment Setting The primary evaluation metric for the success of DQN agents was the mean win-rate against the strong basic opponent (hereafter shortened as SB opponent) in multiple games. Interestingly, possibly due to a lack of augmented exploration, DQN agents benefited from especially long training periods. As such, each agent was trained for a maximum of 100K episodes. Evaluation runs were done every 500 episodes of agent training, as well as at the end of the training. Evaluation statistics were gathered on 200 games on each evaluation. Values are smoothed using exponential moving average.

DQN addition selection Each DQN variant was implemented in their own class, which were then compared in different settings such as using different opponents, a customized action space, utilizing self-play, and using PER. A comparison of the base DQN additions against the SB opponent are provided in Figure 6. As the figure also suggests, our results imply that Double Dueling DQN (hereafter shortened as 3DQN) is a prominent combination of additions. It also succeeds with our other more minor additions, as discussed in later subsections.

Custom action space Each a_i from the discrete action space $\mathcal{A} = \{a_1, ..., a_{|\mathcal{A}|}\}$ used by DQN agents represent a predefined action on hockey environment. The default discrete action space of the hockey environment is limiting with only 7 base movements, representing movement along axes, rotation, and puck shooting. We have expanded the action space to 20 actions in total, which includes combinations of the basic movement primitives. The selected actions are provided in Appendix Section C.2. A comparison of win-rates of 3DQN agents against SB opponent using the default and custom action spaces are provided in Figure 7. The customized action space greatly leverages the agent's performance.

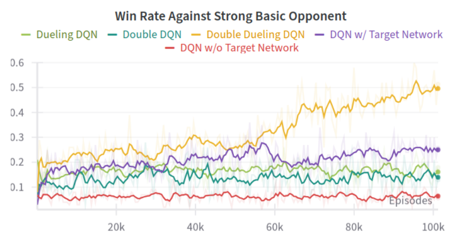

Figure 6: Win rates of base DQN additions vs. SB opponent.

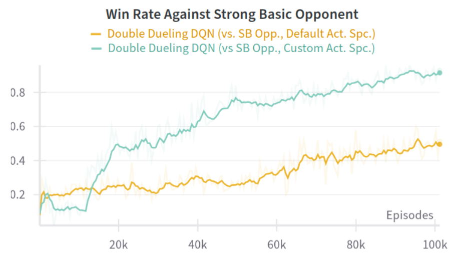

Figure 7: Win rates with different action spaces vs. SB opponent.

Prioritized Experience Replay Our main observation of PER with DQN methods is that it provides a time-wise slower but iteration-wise quicker learning period against a given opponent. Figure 8 compares the learning schedules of two 3DQN agents: One without PER trained for 32 iterations in each episode, and one with PER trained for 4 iterations each episode. It can be seen that PER helps the agent achieve a superior performance in a less number of training iterations.

Self-play Self-play was first implemented as two DQN agents initialized from scratch learning to play against each other. As expected, this led the models to have win-rates near 0.5 against one another, or draw rates near 1.0. Another type-of self play was implemented with POB as introduced in Section 2.1.2: Every 1000 epochs, the opponent buffer was extended with a copy of the current agent if it succeeded against other opponents. Self-play was eventually discarded as both approaches led to worse performance against other players in the tournament, including the basic opponent bots.

Hyperparameter selection 3DQN was decided as the best combination of additions, and the hyperparameters were decided considering this DQN version. **(i)** Experiments with larger layer sizes were conducted: When the layer sizes are increased from 512 to 2048, models show a faster win rate increase but increased overfitting to the trained opponent. **(ii)** To encourage exploration, ϵ-decay was applied in the ϵ-greedy algorithm: Starting with a high value, ϵ was multiplied with a decay rate close to 1 at each episode, until it reached at a predefined minimum. **(iii)** Learning rate was tuned. Among values ranging from $3 \cdot 10^{-6}$ to $3 \cdot 10^{-3}$, a value of $3 \cdot 10^{-5}$ was chosen as optimal based on the win rate against the SB opponent. Other hyperparameters were arbitrarily tuned based on common experience from other available DQN implementations. Final default hyperparameter values are provided in Appendix Section C.1.

Tournament model In the final training, even though the model could easily learn to win against the basic opponents, it struggled against other agents in the tournament. Therefore, a competitive SAC agent from our team was trained against as a representative of real tournament agents. However, as shown in Figure 9, solely training against SAC resulted in a decreased capability against the simple opponents. Therefore, as a simpler alternative to an opponent buffer, the opponent was randomly chosen as the SB opponent or as SAC before each episode during training. It can be seen in the plot that this allowed the model to eventually maintain a high win rate against the SB opponent while learning to win against the more difficult SAC opponent.

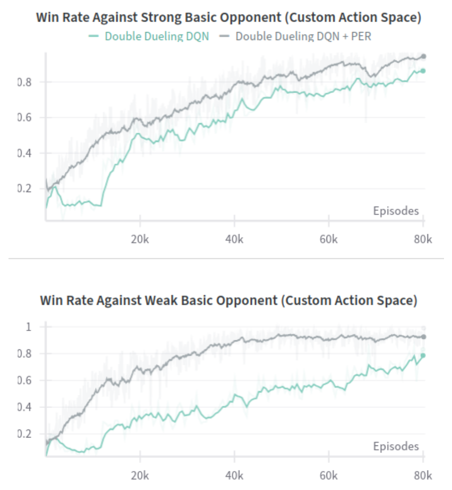

Figure 8: Win rates of 3DQNs with and without PER vs. basic opponents.

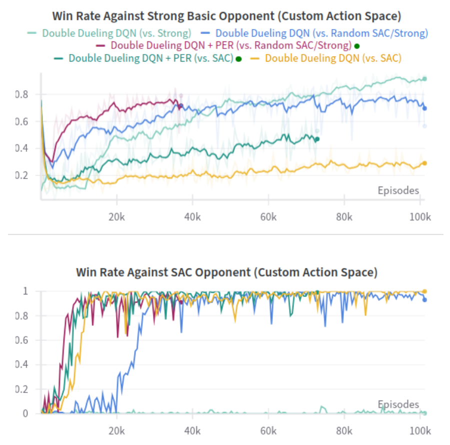

Figure 9: Win rates of 3DQN variations vs. SAC and strong basic opponent. PER runs are cut short due to their slower iterations.

Final Comparison

TD3, DQN, and SAC are all off-policy reinforcement learning algorithms, but they differ fundamentally in how they approach learning. TD3 is designed for continuous action spaces and uses a twin critic network to reduce overestimation bias, along with delayed policy updates to stabilize training. 3DQN is built on DQN and operates in discrete action spaces. It splits action and value function estimators, and avoids overestimation errors in Q-value updates with a modified training objective. SAC, unlike both TD3 and DQN, incorporates entropy maximization into its objective, encouraging exploration by adding a bonus to the reward, which allows it to solve the exploration-exploitation dilemma.

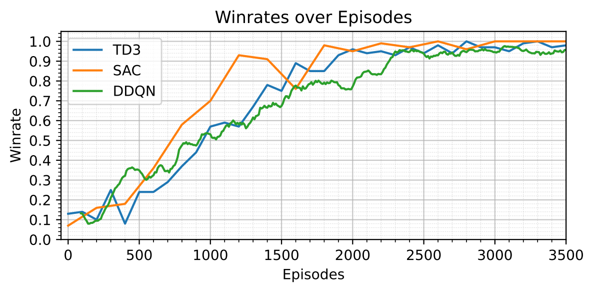

Figure 10: Evaluation win rates against the weak opponent. DQN statistics were scaled from 100K episodes for a clearer comparison.

Figure 10 shows the evaluation win rates over training episodes for all of the reinforcement learning algorithms playing in the hockey environment. All three algorithms successfully learn to play hockey against the weak opponent, eventually achieving near-perfect win rates.

Our SAC model's game play is characterized by quick and direct shots to the opponent net with an aggressive style - however, we lack (1) the ability to execute bank shots where we shoot the puck off the wall to have it bounce toward the net and (2) we are vulnerable to bank shots since we tend to defend our net by getting closer to the opponent.

References

[1] Alain Andres, Esther Villar-Rodriguez, and Javier Del Ser. An Evaluation Study of Intrinsic Motivation Techniques Applied to Reinforcement Learning over Hard Exploration Environments, page 201–220. Springer International Publishing, 2022. ISBN 9783031144639. doi: 10.1007/978-3-031-14463-9_13. URL http://dx.doi.org/10.1007/978-3-031-14463-9_13.

[2] Jimmy Lei Ba, Jamie Ryan Kiros, and Geoffrey E. Hinton. Layer normalization, 2016. URL https://arxiv.org/abs/1607.06450.

[3] Yuri Burda, Harrison Edwards, Amos Storkey, and Oleg Klimov. Exploration by random network distillation, 2018. URL https://arxiv.org/abs/1810.12894.

[4] Onno Eberhard, Jakob Hollenstein, Cristina Pinneri, and Georg Martius. Pink noise is all you need: Colored noise exploration in deep reinforcement learning. In The Eleventh International Conference on Learning Representations, 2023. URL https://openreview.net/forum?id=hQ9V5QN27eS.

[5] Scott Fujimoto, Herke van Hoof, and David Meger. Addressing function approximation error in actor-critic methods, 2018. URL https://arxiv.org/abs/1802.09477.

[6] Tuomas Haarnoja, Aurick Zhou, Pieter Abbeel, and Sergey Levine. Soft actor-critic: Off-policy maximum entropy deep reinforcement learning with a stochastic actor, 2018. URL https://arxiv.org/abs/1801.01290.

[7] Tuomas Haarnoja, Aurick Zhou, Kristian Hartikainen, George Tucker, Sehoon Ha, Jie Tan, Vikash Kumar, Henry Zhu, Abhishek Gupta, Pieter Abbeel, and Sergey Levine. Soft actor-critic algorithms and applications, 2019. URL https://arxiv.org/abs/1812.05905.

[8] L. Kocsis and C. Szepesvári. Discounted ucb. In 2nd PASCAL Challenges Workshop, volume 2, pages 51–134, 2006.

[9] Pawel Ladosz, Lilian Weng, Minwoo Kim, and Hyondong Oh. Exploration in deep reinforcement learning: A survey. Information Fusion, 85:1–22, September 2022. ISSN 1566-2535. doi: 10.1016/j.inffus.2022.03.003. URL http://dx.doi.org/10.1016/j.inffus.2022.03.003.

[10] Clare Lyle, Zeyu Zheng, Khimya Khetarpal, James Martens, Hado van Hasselt, Razvan Pascanu, and Will Dabney. Normalization and effective learning rates in reinforcement learning, 2024. URL https://arxiv.org/abs/2407.01800.

[11] Volodymyr Mnih, Koray Kavukcuoglu, David Silver, Alex Graves, Ioannis Antonoglou, Daan Wierstra, and Martin Riedmiller. Playing atari with deep reinforcement learning, 2013. URL https://arxiv.org/abs/1312.5602.

[12] Tom Schaul, John Quan, Ioannis Antonoglou, and David Silver. Prioritized experience replay, 2016. URL https://arxiv.org/abs/1511.05952.

[13] Hado van Hasselt, Arthur Guez, and David Silver. Deep reinforcement learning with double q-learning, 2015. URL https://arxiv.org/abs/1509.06461.

[14] Che Wang and Keith Ross. Boosting soft actor-critic: Emphasizing recent experience without forgetting the past, 2019. URL https://arxiv.org/abs/1906.04009.

[15] Ziyu Wang, Tom Schaul, Matteo Hessel, Hado van Hasselt, Marc Lanctot, and Nando de Freitas. Dueling network architectures for deep reinforcement learning, 2016. URL https://arxiv.org/abs/1511.06581.

Appendix

A SAC: Architectural and Training Details

A.1 Training Hyperparameters

Table 1 lists the default hyperparameters used during training.

Parameter	**Value**
Number of hidden layers	2
Width of each hidden layer	256
Non-linearity	ReLU
Discount factor (γ)	0.99
Target update rate (τ)	0.005
Target update interval	1
Optimizer	Adam
Number of updates	Same as episode length K
Learning rate (η)	10^{-3}
Entropy coefficient (α)	Auto-tuned
Policy noise	0.2
Noise clip	0.5
Policy frequency	2
Batch size	256
Exploration noise exponent (β)	1.0 (Pink Noise)
Exploration noise deviation (σ)	0.1
Replay buffer size	10^6
D-UCB history window length (τ)	1000
D-UCB bonus factor (ξ)	1
D-UCB discount factor (γ)	0.95
D-UCB reward upper-bound (B)	1

Table 1: Final training hyperparameters.

A.2 Self-Play Algorithm

Our self-play algorithm using POB with D-UCB is as follows:

Algorithm 1 Self-Play with Prioritized Opponent Buffer (D-UCB)

```
1: Initialize agent with parameters $\theta$
2: Initialize D-UCB opponent buffer $\mathcal{B}$ with parameters $(B, \xi, \gamma, \tau)$
3: Add basic opponents to $\mathcal{B}$ (weak, strong, basicshooting, basicdefense) + previous models
4: Initialize replay buffer $\mathcal{R}$
5: for episode $= 1$ to $N$ do
6:     Select opponent $o_k$ from $\mathcal{B}$ using D-UCB sampling
7:     Reset environment, get initial state $s_0$
8:     for $t = 0$ to $T - 1$ do
9:         Select action $a_t \sim \pi_\theta(s_t)$ with exploration noise
10:        Get opponent action $a_t^o \sim \pi_{o_k}(s_t)$
11:        Execute combined action $(a_t, a_t^o)$ in environment
12:        Observe reward $r_t$, next state $s_{t+1}$, and done signal $d_t$
13:        Store transition $(s_t, a_t, r_t, s_{t+1}, d_t)$ in $\mathcal{R}$
14:        if mirror augmentation enabled then
15:            Create mirrored state $\hat{s}_t =$ mirror$(s_t)$
16:            Create mirrored action $\hat{a}_t =$ mirror$(a_t)$
17:            Create mirrored next state $\hat{s}_{t+1} =$ mirror$(s_{t+1})$
18:            Store mirrored transition $(\hat{s}_t, \hat{a}_t, r_t, \hat{s}_{t+1}, d_t)$ in $\mathcal{R}$
19:        end if
20:        Update $s_t \leftarrow s_{t+1}$
21:        if $d_t =$ True then
22:            break
23:        end if
24:    end for
25:    Perform gradient updates on $\theta$ using batches from $\mathcal{R}$
26:    Determine outcome $w \in [0, 1]$ based on win/loss/draw
27:    Update D-UCB statistics for opponent $o_k$ with outcome $w$
28:    if evaluation period and win rate $\geq$ threshold against all opponents then
29:        Create clone of current agent with parameters $\theta$
30:        Add clone to opponent buffer $\mathcal{B}$
31:    end if
32: end for
```

B TD3: Architectural and Training Details

B.1 Training Hyperparameters

Table 2 lists the default hyperparameters used during training.

Parameter	Value
Discount Factor (γ)	0.99
Target Update Rate (τ)	0.005
Policy Noise	0.2
Noise Clip	0.5
Policy Frequency	2
Start Timesteps	1000
Evaluation Frequency	100
Batch Size	2048
Exploration Noise Type	Pink
Exploration Noise Scale	0.1
Pink Noise Exponent	1.0
Pink Noise f_{min}	0.0
Layer Norm ϵ	1×10^{-5}
Save Model Frequency	10 000 episodes
RND Weight	1.0
RND Learning Rate	1×10^{-4}
RND Hidden Dimension	128
Max Episode Steps	600

Table 2: Default training hyperparameters.

B.2 Network Architectures

Actor Network:

- **Input:** State vector (dimension d_{state}).
- **Hidden Layer 1:** Fully-connected layer with 256 units, optionally followed by layer normalization, and a ReLU activation.
- **Hidden Layer 2:** Fully-connected layer with 256 units, optionally followed by layer normalization, and a ReLU activation.
- **Output Layer:** Fully-connected layer mapping to the action vector (dimension d_{action}) with a $\tanh$ activation scaled by the maximum action.

Critic Network:

- Implements two separate Q-networks (denoted as Q1 and Q2) for the purpose of double Q-learning.

- **Input:** Concatenated state and action vector (dimension $d_{\text{state}} + d_{\text{action}}$).
- For each Q-network:
  - **Hidden Layer 1:** Fully-connected layer with 256 units, optionally followed by layer normalization, and a ReLU activation.
  - **Hidden Layer 2:** Fully-connected layer with 256 units, optionally followed by layer normalization, and a ReLU activation.
  - **Output Layer:** Fully-connected layer with 1 unit (Q-value).

RND (Random Network Distillation) Networks:

- Both the target and predictor networks share the same architecture.
- **Architecture:**
  - **Layer 1:** Fully-connected layer from input (state vector, dimension d_{state}) to 128 units, with ReLU activation.
  - **Layer 2:** Fully-connected layer from 128 to 128 units, with ReLU activation.
  - **Layer 3:** Fully-connected layer from 128 to 128 units.

B.3 Additional Details

- **Replay Buffer:** Maintains up to 10^6 transitions for experience replay.
- **Actor and Critic Optimizers:** Both use the Adam optimizer with a learning rate of 3×10^{-4}.
- **Target Networks:** Soft updates are performed using the parameter $\tau = 0.005$.
- **Delayed Policy Updates:** The actor network is updated once every 2 critic updates (i.e., policy frequency is 2).

C DQN: Architectural and Training Details

C.1 Default Training Hyperparameters

Table 3 lists the default hyperparameters used during training.

C.1.1 Network Architecture

All DQN variations except Dueling DQN use the following architecture by default:

- **Q Estimator:** Two fully connected layers of size 512, each followed by ReLU activation. Input size is $d_{\text{observation\_space}}$, output size is $d_{\text{action\_space}}$.

DQN variations using the Dueling DQN algorithm use the following architecture by default:

- **Estimator Backbone:** One fully connected layer of size 512, followed by ReLU activation. Input size is $d_{\text{observation\_space}}$, output size is 512. The output is passed to two separate streams:
- **Advantage (A) Estimator:** Backbone output is passed to two fully connected layers of size 512, followed by ReLU activation. Output size is $d_{\text{action\_space}}$.

Parameter	Value
Learning rate (η)	$3 \cdot 10^{-5}$
Batch size	512
Discount factor (γ)	0.99
Exploration noise type	Uniform
ϵ-greedy exploration probability (ϵ)	0.2
ϵ decay starting value	0.55
ϵ decay rate	0.9995
Target update frequency	every 1000 episodes
Target update rate (τ)	10^{-4}
Evaluation frequency	every 500 episodes
Parameter updates per episode	32
Replay buffer size	10^5

Table 3: Default DQN training hyperparameters.

- **State-value (V) Estimator:** Backbone output is passed to two fully connected layers of size 512, followed by ReLU activation. Output size is 1.
- **Q Estimator Module:** Merges the separate streams: Casts single-dimensional V Estimator output into a vector of length $d_{\text{action\_space}}$ by repeating the value. Estimates the Q function by adding it with the A Estimator output, and subtracting the mean of A Estimator.

C.2 Custom Discrete Action Space

Actions on the hockey environment are represented by a vector of 4 values:

- The first value indicates translation movement on the x axis,
- the second value indicates translation movement on the y axis,
- the third value indicates clockwise or counterclockwise rotation movement,
- and the fourth value indicates shooting a held puck.

In order to keep the action space as simple as possible while providing a flexible set of actions, the action combinations most likely to be used together were considered. Notably, we consider puck shooting only without movement, and omit simultaneous translation and rotation movements. Table 4 lists the extended set of 20 actions of the custom DQN action space.

Action Vector	**Explanation**
`[0., 0., 0., 0.]`	Stand still
`[-1., 0., 0., 0.]`	Move left
`[1., 0., 0., 0.]`	Move right
`[0., -1., 0., 0.]`	Move down
`[0., 1., 0., 0.]`	Move up
`[0., 0., -1., 0.]`	Rotate counterclockwise
`[0., 0., 1., 0.]`	Rotate clockwise
`[-1., -1., 0., 0.]`	Move down-left diagonally
`[-1., 1., 0., 0.]`	Move up-left diagonally
`[1., -1., 0., 0.]`	Move down-right diagonally
`[1., 1., 0., 0.]`	Move up-right diagonally
`[-1., -1., -1., 0.]`	Move down-left diagonally, rotate CCW
`[-1., -1., 1., 0.]`	Move down-left diagonally, rotate CW
`[-1., 1., -1., 0.]`	Move up-left diagonally, rotate CCW
`[-1., 1., 1., 0.]`	Move up-left diagonally, rotate CW
`[1., -1., -1., 0.]`	Move down-right diagonally, rotate CCW
`[1., -1., 1., 0.]`	Move down-right diagonally, rotate CW
`[1., 1., -1., 0.]`	Move up-right diagonally, rotate CCW
`[1., 1., 1., 0.]`	Move up-right diagonally, rotate CW
`[0., 0., 0., 1.]`	Shoot held puck

Table 4: The extended discrete DQN action space.